Radar, lidar, and optical observations in the polar summer mesosphere shortly after a space shuttle launch

M. C. Kelley,[1] M. J. Nicolls,[2] R. H. Varney,[1] R. L. Collins,[3] R. Doe,[2] J. M. C. Plane,[4] J. Thayer,[5] M. Taylor,[6] B. Thurairajah,[3] and K. Mizutani[7]

Received 29 September 2009; revised 4 December 2009; accepted 17 December 2009; published 7 May 2010.

[1] In the summer of 2007, a noctilucent cloud (NLC) campaign was organized in Alaska. Radar, lidar, and photographic methods were used. Due to lighting conditions, the campaign was carried out near the end of the NLC season. Sporadic radar and lidar echoes were obtained until the very end of the campaign, when an exceptionally intense event occurred on the local time night of 10–11 August. This late-season event followed the launch of the space shuttle on 8 August. At least twice before, solstice launches of the shuttle have been followed by unique observations of NLC and sporadic iron layers in the polar regions. This was the case here as well. The iron layer increased in altitude and density, the latter by a factor of 20, compared to the previous night. And, for the first time, (1) polar mesospheric summer echoes (PMSE) were recorded by a radar in an event of this nature and (2) an intense sporadic *E* layer was collocated with the iron atom layer. At the UHF radar frequency used, very large Schmidt numbers are required for PMSE. Indeed, the PMSE was found at and just above the particles responsible for Mie scatter. Such large particles are likely needed to yield large Schmidt numbers. Additionally, similar lidar and sporadic *E* layers were detected over Greenland on the previous night. Here we consider the ion chemistry that could lead to the collocated atom and iron layers and conclude that considerably enhanced water vapor content was required.

Citation: Kelley, M. C., M. J. Nicolls, R. H. Varney, R. L. Collins, R. Doe, J. M. C. Plane, J. Thayer, M. Taylor, B. Thurairajah, and K. Mizutani (2010), Radar, lidar, and optical observations in the polar summer mesosphere shortly after a space shuttle launch, *J. Geophys. Res.*, *115*, A05304, doi:10.1029/2009JA014938.

1. Introduction

[2] On 8 August 2007 at 2236:42 UT, the space shuttle (SST-118) was launched from Cape Kennedy. Independent of this event, several campaigns were being conducted in Greenland and Alaska to study the polar summer mesosphere. Since lidars are an important tool for such studies, lighting conditions in Alaska preclude observations until early August, and by 10 August, the polar mesospheric cloud (PMC) season, also known as noctilucent clouds (NLC), is winding down. Radars do not have a lighting restriction, but our goal was to combine radar, lidar, and optical data, so we concentrated on this period in early August.

[3] The radar used was the Poker Flat Incoherent Scatter Radar (PFISR), a phased array UHF (430 MHz) system operated by SRI International for the National Science Foundation. Only a handful of UHF observations of PMSE exist, and we were anxious to obtain simultaneous radar and lidar data. The University of Alaska operates both a Raleigh/Mie lidar in the green line and a dye-based iron (Fe) resonance lidar at the nearby Davis Optical Observatory.

[4] All of these systems were operational on 11 August 2007 when a spectacular NLC event occurred, by far the best event of the season from many viewpoints. It is this event that we describe here.

[5] Before doing so, we must connect these observations with two other solstice events reported by *Stevens et al.* [2003, 2005]. In each of these cases, a solstice launch of the space shuttle led to bright noctilucent clouds and, in one case, to anomalous iron atom profiles. Such a launch deposits 300 t of water vapor between 100 and 110 km. A mere coincidence between the launches and the observations was ruled out in one case [*Stevens et al.*, 2005] by the fact that the GUVI instrument on the TIMED satellite tracked the water vapor plume from Florida to the southern tip of South America just before the anomalies were detected in Antarctica.

[1]School of Electrical and Computer Engineering, Cornell University, Ithaca, New York, USA.
[2]Center for Geospace Studies, SRI International, Menlo Park, California, USA.
[3]Geophysical Institute, University of Alaska Fairbanks, Fairbanks, Alaska, USA.
[4]School of Chemistry, University of Leeds, Leeds, UK.
[5]Department of Aerospace Engineering Sciences, University of Colorado at Boulder, Boulder, Colorado, USA.
[6]Department of Physics, Utah State University, Logan, Utah, USA.
[7]Environment Sensing and Network Group, National Institute of Information and Communications Technology, Koganei, Japan.

0148-0227/10/2009JA014938

Figure 1. Photograph of noctilucent clouds taken from Donnelly Dome near Fairbanks, Alaska, looking toward the northwest with a wide-angle lens [after *Kelley et al.*, 2009].

Presumably, the iron comes from ablation of the shuttle's main engines.

[6] *Kelley et al.* [2009] have argued that both the rapid polar transport and the rapid expansion of the water vapor plume can be explained by a two-dimensionally turbulent lower thermosphere. Although an interesting and provocative idea, we concentrate here on the local observations in Greenland and Alaska in 2007.

2. Data Presentation

[7] Figure 1 shows the extensive NLC display on the night of 11 August 2007. The clouds filled the sky and exhibited the typical gravity wave-induced structure.

[8] There were no NLCs observed in Alaska after this night and very few previously during the 2007 season. This could be due to lighting conditions, since the Aeronomy of Ice in the Mesosphere (AIM) satellite instruments recorded a typical season (J. Russell, personal communication, 2009). Figure 2 compares the Mie scatter from the mesosphere on two consecutive nights over Alaska, the latter being the night of interest.

[9] The night of 11 August has spectacular echoes, whereas, on the previous night, nothing but noise was observed. Before showing the Alaskan radar data, in Figure 3 we present data from Greenland for the previous night. Greenland, of course, is closer to Florida than Alaska. Shown on the right are Mie scatter echoes from near the mesopause where large NLC particles are located. To the left is an intense sporadic *E* layer about 15 km higher. Without any other data, these observations could be coincidental but, as we shall see, the more comprehensive data set obtained in Alaska the next

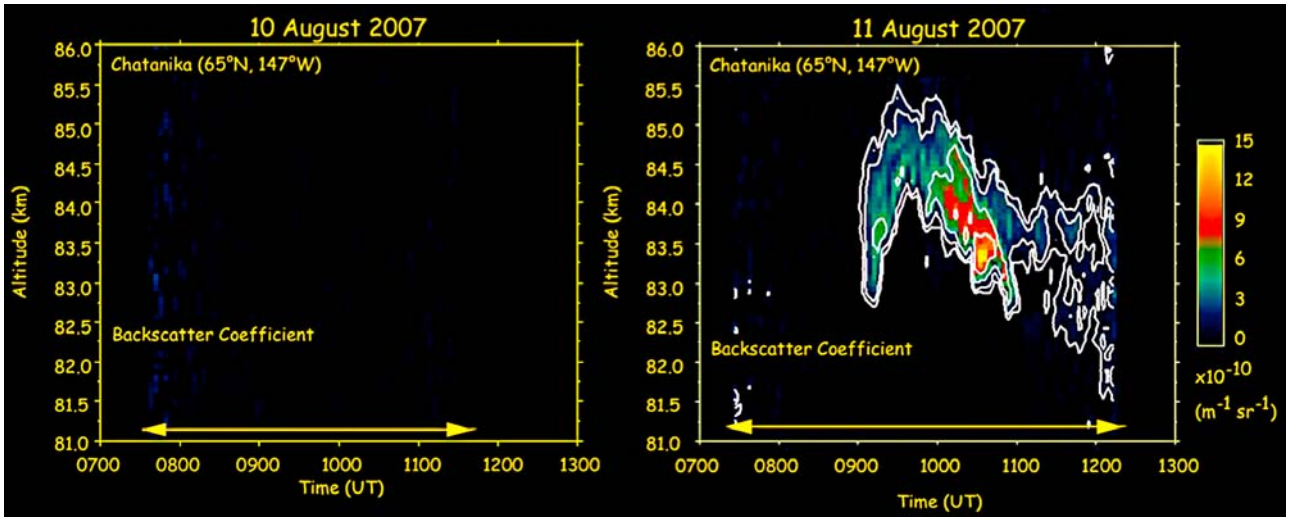

Figure 2. False color plot of the volume backscatter coefficient of noctilucent clouds plotted as a function of time and altitude at Chatanika on 10 and 11 August 2007. The backscatter coefficient is plotted in units of 10^{-10} (m^{-1} sr^{-1}). The horizontal arrows indicate the duration of the observations.

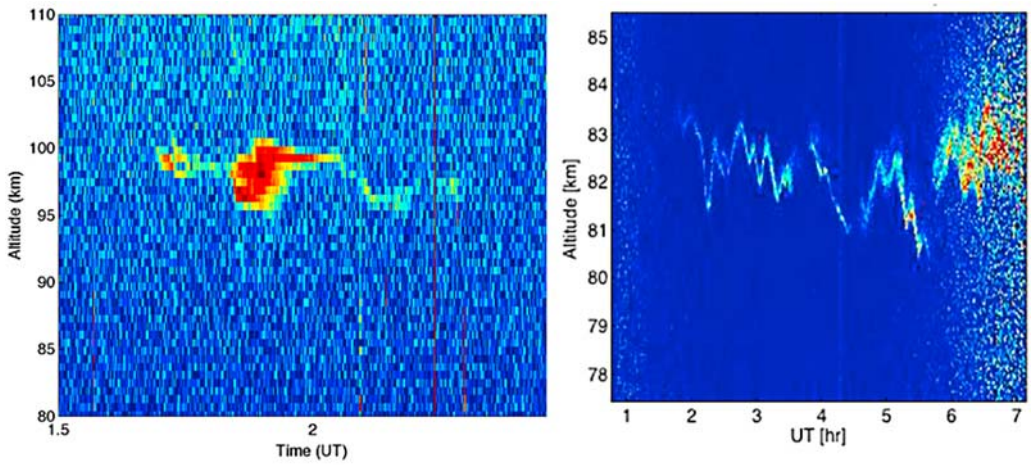

Figure 3. (left) Radar scatter from an intense sporadic *E* layer over the Sondre Stromfjord radar. (right) Simultaneous Mie scatter echoes from noctilucent cloud particles.

day suggests a connection between the shuttle launch, sporadic *E*, the NLC, and iron atom layers.

[10] In Figure 4, we present the UHF radar data for the entire Alaskan data set. The only day with strong PMSE was 11 August 2007 (there may be weak PMSE near 1075–1100 UT on 10 August). We label the mesospheric UHF echoes as PMSE based on their spectral width and on previous studies using PFISR in the International Polar Year [*Nicolls et al.*, 2009; *Varney et al.*, 2009]. It is important to note that the current data were obtained during nighttime and that the nonlayered signals above the PMSE are due to auroral impact ionization. Daytime PMSE, the norm for most PMSE observations, were observed several times in previous PFISR data sets during the summers of 2007 and 2008 [*Nicolls et al.*, 2009; *Varney et al.*, 2009].

[11] Sporadic *E* layers were observed on 30 July, 31 July, 10 August, and 11 August. The layer on 11 August was the longest lived and most prominent, with a peak density of ~3×10^{11} m^{-3}. Next in Figure 5, we show the iron atom layer on two consecutive nights in more detail to emphasize the stark differences. Notice both the unusual intensity and the altitude of the iron layer on 11 August.

[12] The Fe lidar data for 11 August are replotted in Figure 6 and are merged with radar data. In addition, the radar data now show a larger altitude range in Figure 6 (right). In Figure 6 (left), we zoom in on the low-altitude region. The Mie scatter commenced at 0900 UT and grew ever more intense with time. In Figure 6 (right), we show the big picture from the radar standpoint. Auroral precipitation-induced ISR echoes, a sporadic *E* layer, and PMSE are all apparent. Note that, although the lidar echoes became intense after 1000 UT, the radar target did not present until about 1035 UT. The auroral ionization extends below 86 km at nearly the same time. PMSE cannot exist without the ice particles being charged, which in turn requires ionization in the D region, so the occurrence of PMSE at night is often accompanied by auroral ionization [*Varney et al.*, 2009]. In this instance, the PMSE is brightest after the aurora extends below 86 km, but actually began several minutes before the aurora extended. This PMSE was observed in all 26 beams, but a few beams observed a second echo of comparable strength at the same altitude at 1015 UT, long before the aurora extends below 86 km. Thus, one cannot assume a simple, causal relationship between the aurora and the PMSE. The radar data display a better time resolution and demonstrate that at least the ion layer height and density rose almost linearly with time until 0930 UT.

[13] The altitude and peak density of both the atom and ion layers are plotted in Figure 7. The ion density tracked the atom density and overshot it for 20 min. After about 0950 UT, the two plots are nearly identical.

[14] The radar data can be inverted to reveal the precipitating particle energy, as shown in Figure 8. It is well known that electron precipitation is often quite energetic near the dawn terminator. This is the case here. To reach a height of 82 km, the electrons must reach 50 keV.

3. Discussion

3.1. Shuttle-Related Polar Summer Phenomena

[15] We argue here that this event is the third example of polar phenomena following a solstice launch of the space shuttle. The previous two such events were reported by *Stevens et al.* [2003, 2005]. The arguments are summarized as follows: (1) the NLC event was spectacular, even though the time was at the very end of the season, (2) a record iron layer was observed over Alaska, an iron layer similar to those that accompanied another shuttle-related event, and (3) sporadic

Figure 4. PFISR observations during the NLC/PMC/PMSE campaign (30 July to 15 August 2007). A color plot of 2 min, averaged electron density (color scale from 10^{10} to 10^{12} electrons per cubic meter) and 1 h means for three time periods (0750–0850 UT, 0850–0950 UT, and 0950–1050 UT). The only day with strong PMSE was 11 August 2007 (there may be weak PMSE near 1075–1100 UT on 10 August). Sporadic *E* layers were observed on 30 July, 31 July, 10 August, and 11 August. The layer on 11 August was the longest lived and most prominent, with a peak density of ~3×10^{11} m^{-3}.

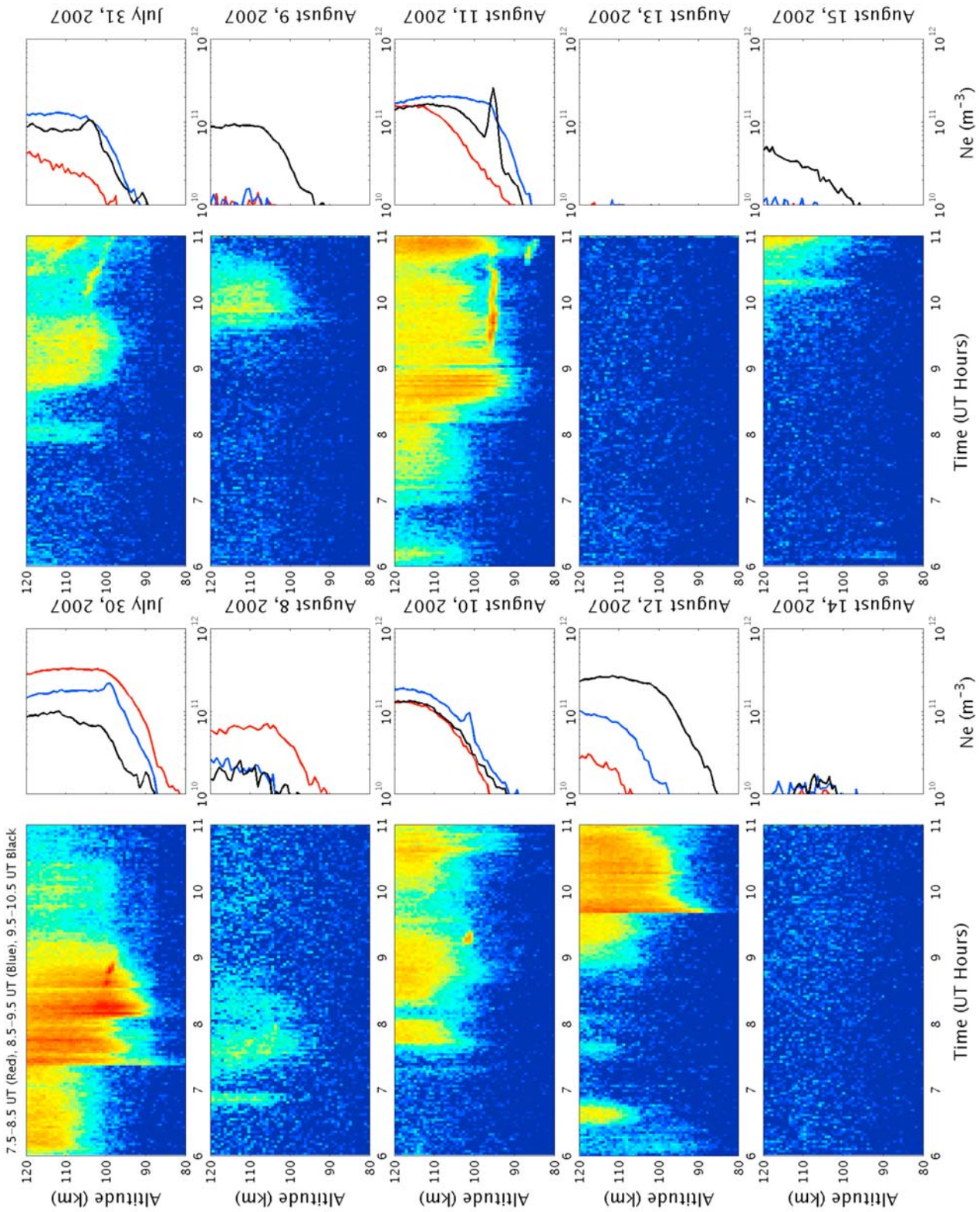
7.5–8.5 UT (Red), 8.5–9.5 UT (Blue), 9.5–10.5 UT Black
Altitude (km)
Time (UT Hours)
Ne (m^{-3})
July 30, 2007
August 8, 2007
August 10, 2007
August 12, 2007
August 14, 2007
July 31, 2007
August 9, 2007
August 11, 2007
August 13, 2007
August 15, 2007

Figure 4

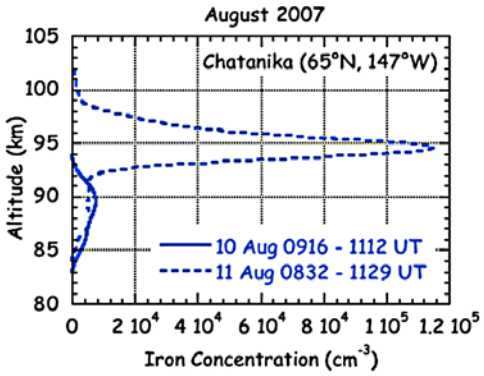

Figure 5. Mesospheric iron concentration profiles as a function of altitude at Chatanika on 10 and 11 August 2007. The profiles represent the average over the observation periods indicated. The data are smoothed with a 5 km Parzen window.

E layers accompanied the iron layer and the NLC events in Alaska and Greenland on the previous night.

[16] In addition to these confirmations of the shuttle launch effects on the polar mesospheric and lower thermospheric (MLT) region, we have a new result, namely, the dense and highly correlated iron atom and sporadic *E* layers. As discussed shortly, to yield these observations, the chemistry of the MLT region requires considerable water vapor, more than natural conditions could provide. This is new and added evidence for the role of shuttle-injected water vapor.

[17] In this section, we must point out the remarkable fact that the shuttle water vapor makes its way to the polar regions from midlatitudes in a day or less, even to the southern polar zone, and that the water vapor plume expands much faster than classical molecular diffusion would suggest. *Kelley et al.* [2009] have suggested that this is an example of (1) an inverse cascade of wind energy to the largest scales in the system and (2) anomalous diffusion of the water vapor plume due to the same physics.

3.2. Fe, Fe+, and the Role of Water Vapor

[18] The lidar observations of Fe and the PFISR measurements of electron density constitute a very unusual data set: a sporadic neutral Fe layer with some of the highest Fe densities ever measured in the atmosphere (peaking at around 1.12×10^5 cm^{-3}), and a sporadic *E* layer, which coincides both spatially and temporally with the Fe layer and contains a similar concentration of electrons at a relatively low altitude of around 95 km. As we will show, these observations place tight constraints on a model of the metallic ion chemistry and provide strong evidence for the presence of large

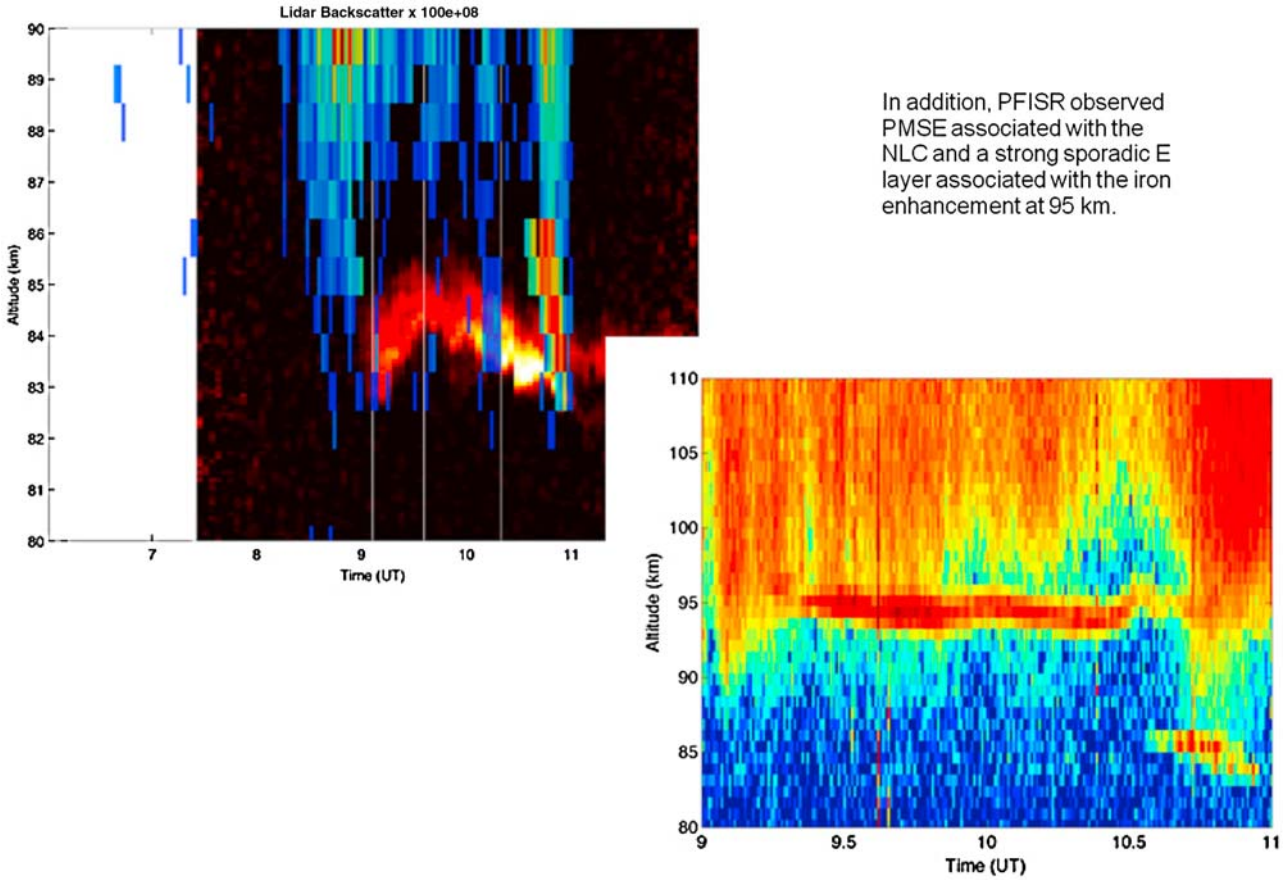

Figure 6. (left) The lidar and radar data are superposed for heights below 90 km. (right) A larger height range for the radar signal is plotted. Note the radar echo near 85 km in both panels. In Figure 6 (left), the most intense radar echo is seen at and just above the lidar echo.

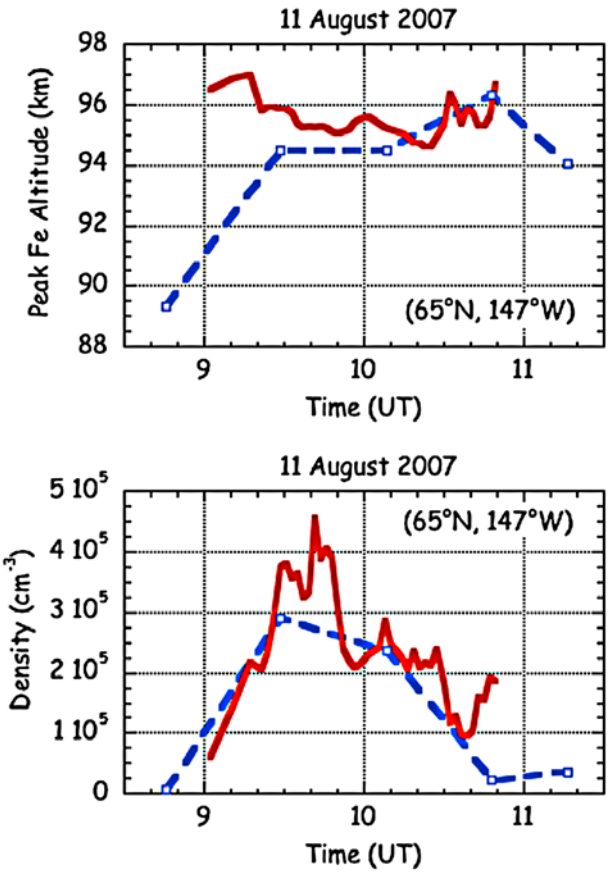

Figure 7. Evolution of neutral and ion Fe layers at Chatanika on 11 August 2007. (top) Peak density of neutral (blue dashed line with squares) and ion (red solid line) layers as a function of time. (bottom) Altitude of the neutral peak density (blue dashed line with squares) and ion (red solid line) density as a function of time.

quantities of H_2O, which would be present from a shuttle exhaust plume.

[19] Table 1 lists the important ion-molecule reactions of Fe^+ in the MLT region. These reactions have all been studied now in the laboratory, apart from the dissociative electron recombination reaction (reaction R11). However, the rate coefficient k_{11} for this class of reactions can be estimated to better than a factor of 2 by comparison with the measured rate coefficients for dissociative recombination of ions such as NO^+ and O_2^+ [*Florescu-Mitchell and Mitchell*, 2006]. Fe^+ ions form rapidly by charge transfer with ambient NO^+ and O_2^+ ions (R1 and R2). The chemical lifetime of Fe^+ then depends on the efficiency with which Fe^+ can be neutralized to Fe. Radiative recombination with electrons ($Fe^+ + e^- \rightarrow Fe + h\nu$) is an inefficient process [*Vondrak et al.*, 2006]. However, below 110 km, the concentrations of O_3, O_2, and N_2 are sufficiently large for ion-molecule chemistry to become important: molecular ions of Fe^+ form primarily through R3, R4, and R5 and, to a lesser extent, through R6 and R7 [*Vondrak et al.*, 2006]. Normally, formation of FeO^+ through R3 dominates above 85 km because the low atmospheric density constrains the termolecular reactions R4–R7 [*Rollason and Plane*, 1998]. The resulting molecular ions can then undergo dissociative recombination with electrons. If the combination of R3–R7 could occur unchecked, then Fe^+ ions at 95 km would have a lifetime of only ~30 s. Crucially, atomic O destroys these molecular ions through reactions R8–R10 [*Woodcock et al.*, 2006].

[20] Inspection of Figure 8 shows that, between about 0930 and 1030 h, a pronounced sporadic *E* layer occurred at 95 km with a peak electron concentration of ~3×10^5 cm^{-3}. This period did not coincide with the highest levels of auroral precipitation (Figure 8), so the ions in this sporadic *E* layer were relatively long lived; that is, this was a classic sporadic layer composed mostly of metallic ions.

[21] Figure 7 shows that the sporadic Fe layer decreased to background levels below 93 km and above 98 km. The electron concentrations at these altitudes were [e^-] ~7×10^4 cm^{-3}, and presumably, the dominant positive ion was NO^+ in the absence of elevated metallic concentrations

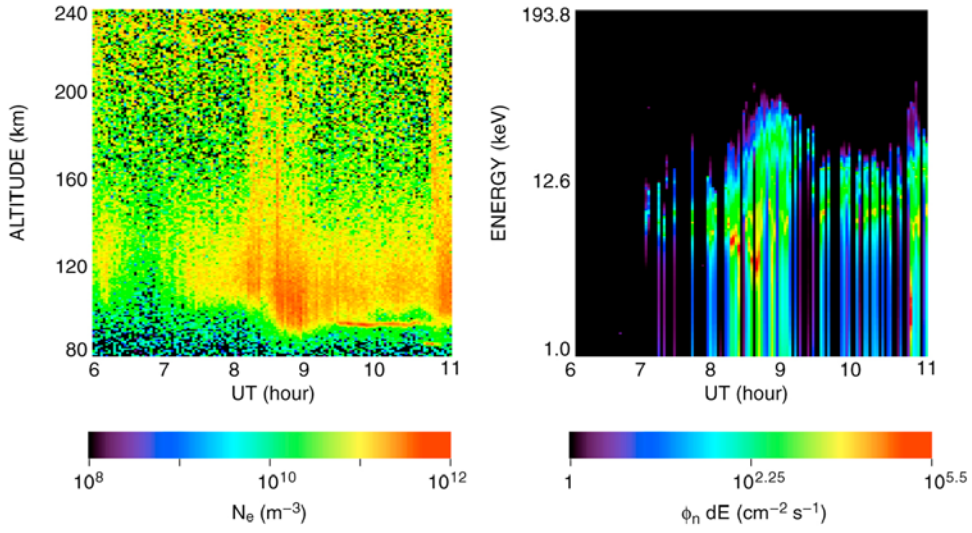

Figure 8. Electron density and the flux/energy of precipitating particles needed to attain these densities.

Table 1. Ion-Molecule Chemistry of Iron in the MLT

Reaction Number	Reaction	Rate Coefficient[a]	Source[b]
R1	$Fe + NO^+ \rightarrow Fe^+ + NO$	9.2×10^{-10}	b
R2	$Fe + O_2^+ \rightarrow Fe^+ + O_2$	1.1×10^{-9}	b
R3	$Fe^+ + O_3 \rightarrow FeO^+ + O_2$	$7.1 \times 10^{-10}\ e^{-(130/T)}$	c
R4	$Fe^+ + O_2(+M) \rightarrow Fe^+.O_2(M = N_2, O_2)$	$8.4 \times 10^{-30}\ (T/300\ K)^{-1.86}$	c
R5	$Fe^+ + N_2(+M) \rightarrow Fe^+.N_2$	$4.0 \times 10^{-30}\ (T/300\ K)^{-1.52}$	c
R6	$Fe^+ + CO_2(+M) \rightarrow Fe^+.CO_2$	$2.0 \times 10^{-29}\ (T/300\ K)^{-2.31}$	d
R7	$Fe^+ + H_2O(+M) \rightarrow Fe^+.H_2O$	$1.1 \times 10^{-28}\ (T/300\ K)^{-2.02}$	d
R8	$Fe^+.N_2 + O \rightarrow FeO^+ + N_2$	4.6×10^{-10}	e
R9	$Fe^+.O_2 + O \rightarrow FeO^+ + O_2$	6.3×10^{-11}	e
R10	$FeO^+ + O \rightarrow Fe^+ + O_2$	3.2×10^{-11}	e
R11	$Fe^+.X + e^- \rightarrow Fe + X(X = O, O_2..)$	$3.0 \times 10^{-7}\ (200/T)^{1/2}$	f

[a]Units are as follows: bimolecular, $cm^3\ molecule^{-1}\ s^{-1}$; termolecular, $cm^6\ molecule^{-2}\ s^{-1}$.
[b]Sources are as follows: b, *Rutherford and Vroom* [1972] ; c, *Rollason and Plane* [1998] ; d, *Vondrak et al.* [2006]; e, *Woodcock et al.* [2006] ; f, estimate based on dissociative recombination of NO^+ and O_2^+ ions.

[*Grebowsky and Aikin*, 2002]. This implies that the ion pair production rate was around 2000 $cm^{-3}\ s^{-1}$ ($= k_{\|}[e^{-2}]$). The typical atmospheric conditions at 95 km for this location and time, as predicted from models such as MesoMOD [*Murray and Plane*, 2005], are: $[M] = 1.0 \times 10^{13}\ cm^{-3}$; $[O_3] = 1.8 \times 10^8\ cm^{-3}$; $[O] = 5.4 \times 10^{11}\ cm^{-3}$; $[H_2O] = 4.2 \times 10^7\ cm^{-3}$; $[CO_2] = 1.6 \times 10^{10}\ cm^{-3}$. Under these conditions, the modeled ratio of $[e^-]/[Fe] = 1.1 \times 10^5/3.0 \times 10^5 = 0.37$. This is significantly smaller than the measured ratio of 1.0 (see above). In this case, the two major positive ions are $[Fe^+] = 6.9 \times 10^4\ cm^{-3}$ and $[NO^+] = 4.3 \times 10^4\ cm^{-3}$.

[22] Since reaction R3 normally controls the rate of conversion of Fe^+ to Fe at 95 km, the most likely explanation for this discrepancy is that O_3 has been substantially depleted. In fact, in order to produce the observed $[e^-]/[Fe]$ ratio of 1.0 *and* their absolute concentrations, O_3 needs to have been depleted by at least a factor of 50. The modeled [Fe] is then $3.0 \times 10^5\ cm^{-3}$, and the two major positive ions are $[Fe^+] = 2.8 \times 10^5\ cm^{-3}$ and $[NO^+] = 0.2 \times 10^5\ cm^{-3}$.

[23] The most likely way for this to occur is through odd-hydrogen chemistry:

$$H + O_3 \rightarrow OH + O_2$$

$$O + OH \rightarrow H + O_2$$

$$\text{Net:}\ \ O + O_3 \rightarrow 2O_2.$$

Elevated H and OH are readily produced from Lyman-α photolysis of H_2O. Using the MesoMOD 1-D model, *Murray and Plane* [2005] demonstrated that an increase in H_2O by a factor of 100 would lead to a 50-fold depletion of O_3 in only 36 h for the August conditions at 65°N. Such elevated H_2O levels are consistent with shuttle plumes [*Stevens et al.*, 2005].

3.3. Nighttime, Aurorally Induced PMSE

[24] Observations of PMSE at night are very rare, as are UHF PMSE at any time. PMSE require the presence of large charged particles to raise the Schmidt number. The particles are certainly large enough to support PMSE because the lidar detects Mie scatter. How the particles become charged while not sunlit and before the aurora penetrates to the PMSE altitude is more difficult to explain.

[25] Typically, the ice layer will extend up to ~90 km, with the smallest particles near the top [*Rapp and Thomas*, 2006]. These small particles are impossible to detect with a lidar. Between 0830 and 0900 UT, the auroral ionization extends as low as 88 km, meaning that the aurora could have charged these smaller particles if they were present. The particles near the top of the cloud will sediment downward, coagulating into larger particles as they fall. The terminal velocity of a spherical particle is given by

$$v_{sedi} = \frac{\rho g r}{2 n_a} \sqrt{\frac{\pi}{2 m_a k_B T}} \cdot \left(1 + \frac{\eta}{2} - \frac{\eta'}{2} + \frac{\pi}{8}\eta'\right)^{-1},$$

where ρ is the density of the particle, g is the acceleration due to gravity, r is the particle radius, n_a is the neutral air density, m_a is the mass of an air molecule, and η and η' are the accommodation coefficients for the tangential and normal components of the momentum, respectively [*Turco et al.*, 1982; *Rapp and Thomas*, 2006]. The accommodation coefficients are not well known, but they must be between 0 and 1, so the final term is between 0.7 and 1. Taking this final term to be 1 and assuming a particle density of $2\ g/cm^3$, a neutral density of $10^{20}\ m^{-3}$, and a temperature of 130 K, a 10 nm particle will take ~2 h to fall 1 km. Clearly, if there is a downward wind, the particle can move much faster than this. The particles responsible for the Mie scatter descend 1 km in only 1 h between 0930 and 1030 UT, which is faster than these particles would be expected to fall due to gravity alone. Thus, it is plausible that small particles that were charged by the aurora above 88 km could have been transported down to ~85 km a few hours later. As the particles descend and coagulate, they have no way to lose their charge because they cannot be photoionized in darkness, and secondary electron emission is unlikely to be significant.

4. Conclusions

[26] Once again [*Stevens et al.*, 2003, 2005], a space shuttle launch at solstice has created observable changes in the polar upper atmosphere. In this case, the phenomena were observed with a complete suite of instruments: three lidars, two UHF radars, and a wide-angle camera. In the Greenland sector, the radar detected a strong sporadic *E* layer at the same time that the Rayleigh lidar detected large particles near 82 km. The former might have been thought to be a coincidence. How-

ever, the combined radar and lidar data in Alaska, coupled with the theoretical work reported here, shows that the atom and ion layers are intimately related and that the latter is made up of iron ions. Furthermore, the nearly equal and long-lasting atom/iron layers depend on being collocated with water vapor, which mediates their interaction.

[27] After three events of this type, it is clear that the shuttle burn releases huge amounts of water vapor and iron atoms into the lower thermosphere. Remarkably, this material rapidly makes its way to the polar regions. Once there, for a solstice launch, the water vapor forms huge noctilucent cloud displays in addition to the atom and iron layers. During other seasons, such a launch should lead to the atom and iron layers but not the NLC due to the requirement of very low mesopause temperatures.

[28] The rapid transport to the poles is remarkable and shows that we do not understand the circulation of the lower thermosphere. A new idea is that the region acts as a two-dimensionally turbulent fluid [*Kelley et al.*, 2009].

[29] **Acknowledgments.** Work at Cornell University was supported by National Science Foundation grants ATM-0551107 and ATM-00538343. Work at the University of Alaska Fairbanks was supported by NSF grants ARC-0632387 and ATM-514103. Work at the University of Colorado at Boulder was supported by NSF grant ATM-0454999. The authors thank the staff at Poker Flat Research Range and the Sondrestrom Atmospheric Research Facility for their support.

[30] Amitava Bhattacharjee thanks the reviewers for their assistance in evaluating this paper.

References

Florescu-Mitchell, A. I., and J. B. A. Mitchell (2006), Dissociative recombination, *Phys. Rep.*, *430*, 277–374.

Grebowsky, J. M., and A. C. Aikin (2002), In situ measurements of meteoric ions, in *Meteors in the Earth's Atmosphere*, edited by E. Murad and I. P. Williams, pp. 189–214, Cambridge Univ. Press, Cambridge, U. K.

Kelley, M. C., C. E. Seyler, and M. F. Larsen (2009), Two-dimensional turbulence, space shuttle plume transport in the thermosphere, and a possible relation to the Great Siberian Impact Event, *Geophys. Res. Lett.*, *36*, L14103, doi:10.1029/2009GL038362.

Murray, B. J., and J. M. C. Plane (2005), Modelling the impact of noctilucent cloud formation on atomic oxygen and other minor constituents of the summer mesosphere, *Atmos. Chem. Phys.*, *5*, 1027–1038.

Nicolls, M. J., M. C. Kelley, R. H. Varney, and C. J. Heinselman (2009), Spectral observations of polar mesospheric summer echoes at 33 cm (450 MHz) with the Poker Flat Incoherent Scatter Radar, *J. Atmos. Sol. Terr. Phys.*, *71*, 662–674, doi:10.1016/j.jastp.2008.04.019.

Rapp, M., and G. E. Thomas (2006), Modeling the microphysics of mesospheric ice particles: Assessment of current capabilities and basic sensitivities, *J. Atmos. Sol. Terr. Phys.*, *68*, 715–744, doi:10.1016/j.jastp.2005.10.015.

Rollason, R. J., and J. M. C. Plane (1998), A study of the reactions of Fe^+ with O_3, O_2 and N_2, *J. Chem. Soc. Faraday Trans.*, *94*, 3067–3075, doi:10.1039/a805140b.

Rutherford, J. A., and D. A. Vroom (1972), Formation of iron ions by charge transfer, *J. Chem. Phys.*, *57*, 3091–3093, doi:10.1063/1.1678724.

Stevens, M. H., J. Gumbel, C. R. Englert, K. U. Grossmann, M. Rapp, and P. Hartogh (2003), Polar mesospheric clouds formed from space shuttle exhaust, *Geophys. Res. Lett.*, *30*(10), 1546, doi:10.1029/2003GL017249.

Stevens, M. H., R. R. Meier, X. Chu, M. T. DeLand, and J. M. C. Plane (2005), Antarctic mesospheric clouds formed from space shuttle exhaust, *Geophys. Res. Lett.*, *32*, L13810, doi:10.1029/2005GL023054.

Turco, R. P., O. B. Toon, R. C. Whitten, R. G. Keesee, and D. Hollenbach (1982), Noctilucent clouds: Simulation studies of their genesis, properties and global influences, *Planet. Space Sci.*, *30*, 1147–1181, doi:10.1016/0032-0633(82)90126-X.

Varney, R. H., M. J. Nicolls, C. J. Heinselman, and M. C. Kelley (2009), Observations of polar mesospheric summer echoes using PFISR during the summer of 2007, *J. Atmos. Sol. Terr. Phys.*, *71*, 470–476, doi:10.1016/j.jastp.2009.01.002.

Vondrak, T., K. R. I. Woodcock, and J. M. C. Plane (2006), A kinetic study of the reactions of Fe^+ with N_2O, N_2, O_2, CO_2 and H_2O, and the ligand-switching reactions $Fe^+ \cdot X + Y \rightarrow Fe^+ \cdot Y + X$ ($X = N_2, O_2, CO_2$; $Y = O_2, H_2O$), *Phys. Chem. Chem. Phys.*, *8*, 503–512, doi:10.1039/b508922k.

Woodcock, K. R. S., T. Vondrak, S. R. Meech, and J. M. C. Plane (2006), A kinetic study of the reactions $FeO^+ + O$, $Fe^+ \cdot N_2 + O$, $Fe^+ \cdot O_2 + O$ and $FeO^+ + CO$: Implications for sporadic *E* layers in the upper atmosphere, *Phys. Chem. Chem. Phys.*, *8*, 1812–1821, doi:10.1039/b518155k.

R. L. Collins and B. Thurairajah, Geophysical Institute, University of Alaska Fairbanks, Fairbanks, AK 99775, USA.

R. Doe and M. J. Nicolls, Center for Geospace Studies, SRI International, Menlo Park, CA 94025, USA.

M. C. Kelley and R. H. Varney, School of Electrical and Computer Engineering, Cornell University, Ithaca, NY 14853, USA. (mck13@cornell.edu)

K. Mizutani, Environment Sensing and Network Group, National Institute of Information and Communications Technology, 4-2-1 Nukui-kita, Koganei, Tokyo 184-8795, Japan.

J. M. C. Plane, School of Chemistry, University of Leeds, Leeds LS2 9JT, UK.

M. Taylor, Department of Physics, Utah State University, Logan, UT 84322, USA.

J. Thayer, Department of Aerospace Engineering Sciences, University of Colorado at Boulder, Boulder, CO 80309, USA.